Pre-Clinical Research Report

Journal of INTERNATIONAL MEDICAL RESEARCH

Journal of International Medical Research
2018, Vol. 46(11) 4717–4721

DOI: 10.1177/0300060518796388
journals.sagepub.com/home/imr
SAGE

Characteristics of wooden intraocular foreign body by magnetic resonance imaging in rabbits

Baohong Wen[1], Jingliang Cheng[1], Huixia Zhang[1], Yong Zhang[1], Xiaonan Zhang[1], Chenyu Yan[1] and Fengguang Zhang[2]

Abstract

Objective: Intraocular foreign body (IOFB), a frequent cause of ocular trauma, causes serious damage to the eyes. This study was designed to elaborate and compare the characteristics of different magnetic resonance imaging (MRI) sequences in detecting wooden IOFBs in rabbits.

Methods: The right vitreous of 24 healthy rabbits was randomly implanted with diverse wooden foreign bodies (diameter $\varphi = 0.2$ mm). The T_1-weighted imaging (T_1WI), T_2-weighted imaging (T_2WI), proton density-weighted imaging (PDWI), and susceptibility-weighted imaging (SWI) sequences were applied individually 2 weeks after the implantation.

Results: IOFBs were detected as linear low signals on T_1WI, T_2WI, PDWI, and SWI (SWI image). The detectable rates of poplar wood with a length of 0.5 mm were 0%, 50%, 0%, and 67% for T_1WI, T_2WI, PDWI, and SWI, respectively. SWI and T_2WI sequences exhibited higher sensitivity than T_1WI and PDWI. The detectable rates of the first three SWI sequences (magnitude, phase, and SWI) were all 67%, which was higher than that of the minimum intensity projection sequence (33%).

Conclusion: MRI is practicable in the diagnosis of wooden IOFBs. SWI and T_2WI are optimal for the integrated diagnosis of wooden IOFBs and could be used for diagnosis and immediate treatment.

Keywords

Intraocular foreign body, vitreous body, magnetic resonance imaging, susceptibility-weighted imaging, rabbit model, ocular trauma

Date received: 31 October 2017; accepted: 2 August 2018

[1]Department of MRI, The First Affiliated Hospital of Zhengzhou University, Zhengzhou, P. R. China
[2]Department of Radiology, Henan Tumor Hospital, Zhengzhou, P. R. China

Corresponding author:
Jingliang Cheng, Department of MRI, The First Affiliated Hospital of Zhengzhou University, No. 1 Jianshe East Road, Zhengzhou, Henan Province 450052, P. R. China.
Email: chengjingliang126@126.com

Introduction

Without immediate treatment, an intraocular foreign body (IOFB) will cause serious damage to the eyes. Residual IOFBs are prone to continuously affect the intraocular system, increasing the risk of infection and complications such as endophthalmitis, traumatic cataract, and vitreous opacity.[1] In recent years, the diagnostic accuracy of IOFBs has been drastically improved by the widespread application of X-ray computed tomography (CT), magnetic resonance imaging (MRI), and ultrasonography.[2]

Based on the T_2*-weighted gradient echo sequence, susceptibility-weighted imaging (SWI) enhances the diagnostic accuracy among objects with different magnetic susceptibilities.[3] However, few reports are available for validating the diagnostic value of this sequence for IOFBs. Therefore, the present study was designed to elaborate and compare the characteristics of different MRI sequences [i.e., T_1-weighted imaging (T_1WI), T_2-weighted imaging (T_2WI), proton density-weighted imaging (PDWI) and SWI] in detecting wooden IOFBs.

Materials and methods

Animals and wooden IOFBs

Twenty-four healthy male Japanese rabbits (2.0–2.5 kg in body weight, normal binocular vision) were purchased from Henan Kangda Laboratory Animal Co., Ltd. (Zhengzhou, China). This study was approved by the Animal Care and Use Ethics Committee of The First Affiliated Hospital of Zhengzhou University. All animal-handling procedures were performed according to the Guide for the Care and Use of Laboratory Animals of the National Institutes of Health and followed the guidelines of the Animal Welfare Act. Xylem of poplar (Salicaceae, timber) was selected as the IOFB for implantation after being trimmed into cylinders ($\varphi = 0.2$ mm; length = 0.2, 0.5, 1.0, and 2.0 mm) as gauged with a vernier caliper. Xylem from a fresh branch was defined as a wet IOFB, and xylem that had been air-dried for 1 month was defined as a dry IOFB.

Animal models

The experimental animals underwent fasting and water deprivation 8 hours before the implantation. Chloral hydrate (10%, 0.3 g/kg) was transperitoneally injected to induce general anesthesia. The rabbit was maintained in the left lateral position on the experimental table after anesthesia. The avascular area of the conjunctival layer, 3 mm above the corneal limbus of the right eye, was cut with sterilized eye scissors. The white sclera was fully exposed and then punctured with a 1-mL sterile syringe. The wooden IOFB was then lowered into the vitreous cavity with ophthalmic forceps, and the puncture site was sewn with 8-0 absorbable sutures. Ofloxacin ointment was applied onto the injured right eye. The rabbits were fed for 2 weeks, and the MRI examination was then repeated.

MRI examinations

All experiments were conducted on Siemens 3.0T Verio Scanner System (Siemens Medical Solutions, Erlangen, Germany). The head of each rabbit was centered on the dedicated coil (Shanghai Chenguang Medical Instrument Co., Ltd., Shanghai, China) in the prone position to maintain a downward gaze, and three-dimensional positioning images (transverse, sagittal, and coronal planes) were obtained. Scanning in the axial, oblique sagittal, and coronal directions was performed successively on the whole eye socket. The baseline of the transverse scan was perpendicular to the hard palate, while that of the oblique

sagittal and coronal scans was parallel to the optic nerve and the hard palate, respectively. The scanning sequences in this study were T_1WI, T_2WI, PDWI, and SWI. All original data and images were sent to the Siemens 3.0T Syngo post-processing workstation (Siemens Medical Solutions) to record the number of identified IOFBs, any complications, the observed diameters, and the calculated magnitude (Mag) value, phase (Pha) value, minimum intensity projection (mIP) value, and SWI value.

Statistical analysis

SPSS for Windows, version 16.0 (SPSS Inc., Chicago, IL, USA) was used for the statistical analysis (at the 5% significance level). Linear trends between the detectable rates of IOFB (same material) and the IOFB length were assessed by the chi-square test for trend. The one-sample *t* test was performed to compare differences between the actual diameter and the diameter observed by different MRI sequences.

Results

MRI manifestation of wooden IOFBs in rabbit vitreous

All poplar IOFBs implanted in rabbit vitreous typically produced punctate and/or linear low signals on T_1WI (Figure 1(a)), T_2WI (Figure 1(b)), PDWI (Figure 1(c)), the Mag image (Figure 1(d)), the mIP image (Figure 1(e)), and the SWI image (Figure 1(f)) but presented mixed signals on the Pha image (Figure 1(g)). The detectable length was 2.0 mm for T_1WI, 1.0 mm for PDWI, and 0.5 mm for both T_2WI and SWI sequences, indicating that the sensitivities of T_2WI and SWI were higher than those of T_1WI and PDWI (Table 1).

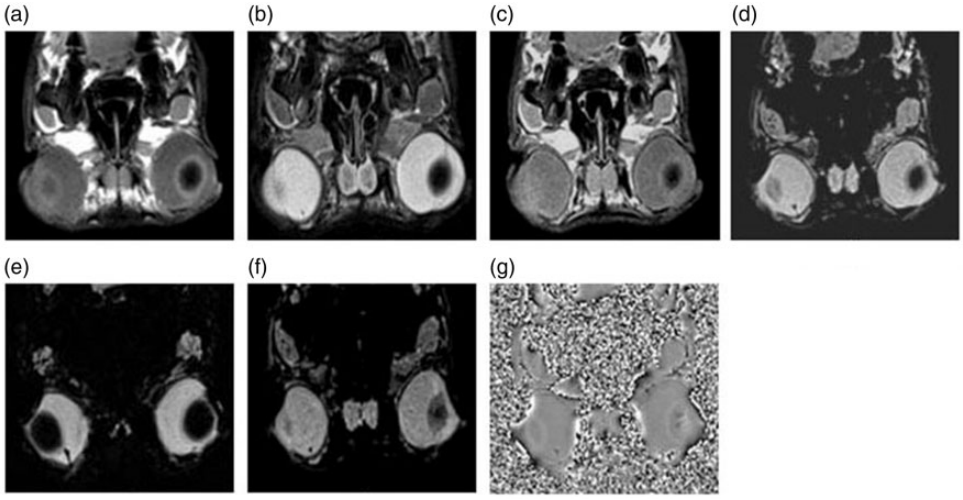

Figure 1. Transverse MRI images of rabbit vitreous implanted with dry poplar (length = 1.0 mm) for 2 hours. (a–g) T_1WI image, T_2WI image, PDWI image, Mag image, mIP image, SWI image, and Pha image, respectively. (a, c) No abnormalities were found in the vitreous. The detected foreign bodies presented punctate or linear low signals in (b) and (d–f) and mixed signals in (g). MRI, magnetic resonance imaging; T_1WI, T_1-weighted imaging; T_2WI, T_2-weighted imaging; PDWI, proton density-weighted imaging; Mag, magnitude; mIP, minimum intensity projection; SWI, susceptibility-weighted intensity; Pha, phase.

Table 1. Detection rate of wooden foreign bodies by T_1WI, T_2WI, PDWI, and SWI (n = 6).

Length (mm)	T_1WI	T_2WI	PDWI	SWI
0.2	0%	0%	0%	0%
0.5	0%	50%	0%	67%
1.0	0%	50%	17%	100%
2.0	17%	100%	33%	100%

T_1WI, T_1-weighted imaging; T_2WI, T_2-weighted imaging; PDWI, proton density-weighted imaging; SWI, susceptibility-weighted imaging.

Table 2. Detection rate of wooden foreign bodies by different SWI sequences (n = 6).

Length (mm)	Mag	Pha	mIP	SWI
0.2	0%	0%	0%	0%
0.5	67%	67%	33%	67%
1.0	100%	100%	100%	100%
2.0	100%	100%	100%	100%

Mag, magnitude; Pha, phase; mIP, minimum intensity projection; SWI, susceptibility-weighted imaging.

Comparison of detectable rates by different SWI sequences

As revealed in Table 2, the Mag image, Pha image, mIP image, and SWI image could detect IOFBs with a length of 0.5, 1.0, and 2.0 mm. The detectable rates of the Mag image, Pha image, and SWI image were identical (67%), while that for the mIP image was 33%.

Discussion

Wooden IOFBs can cause a rapidly healing wound at the surface, leaving residual foreign material in the wound and inducing subsequent misdiagnosis.[4] One study showed that non-magnetic low-density IOFBs were misdiagnosed by CT but confirmed by MRI.[5] Wooden IOFBs are hardly detected by CT and occasionally misdiagnosed as air.[6] MRI has been widely applied for the performance of multidimensional imaging with higher resolution, allowing for the detection of the amount and location of wooden IOFBs in addition to common complications (e.g., vitreous hemorrhage). Hence, MRI is effective and efficient in diagnosing and localizing IOFBs, particularly wooden IOFBs.

SWI is one such technique that takes advantage of the magnetic property to create useful image contrast. SWI combines information from both Mag and Pha images from a T2*-weighted gradient echo sequence, further enhancing the susceptibility effect and thus improving the detection sensitivity.[7] In the present study, the detected IOFBs on the conventional MRI sequences (T_1WI, T_2WI, and PDWI) presented punctate and/or linear low signals, the shape of which depended on the implanted direction and scanning section. Because of the small size of the wooden IOFBs in this study, the magnetic signals of the vitreous did not obviously change. The rabbit vitreous presented low signals on T_1WI, indicating that the T_1WI sequence was inappropriate for imaging the wood IOFBs. T_2WI was conducive to detection of the wooden IOFBs. Signals of vitreous on PDWI were slightly higher than those on T_1WI. SWI indicated the maximal detectable rate. Length is critical for the detectability of wooden IOFBs by SWI and should be further studied in larger samples under different space resolutions.

Notably, our rabbit study model is somewhat different from the human eye; the rabbit vitreous volume is smaller (human vitreous, 4.5 mL versus rabbit vitreous, 1.5 mL), the lens is larger, and the retina is thinner, avascular, and has no fovea. Therefore, the sensitivity of MRI in human eyes may differ from that in rabbit eyes, and data from clinical trials are needed to characterize human eyes. However, our data show that the SWI scanning sequence can help to improve the detectable rates of wooden IOFBs and thus has specific clinical application value.

Declaration of conflicting interest

The authors declare that there is no conflict of interest.

Funding

This study was granted by Basic and Advanced Technology Research Project, Department of Science and Technology of Henan Province (No. 122300410364).

References

1. Qi Y, Zhang FY, Peng GH, et al. Characteristics and visual outcomes of patients hospitalized for ocular trauma in central China: 2006–2011. *Int J Ophthalmol* 2015; 8: 162–168.
2. Wen B, Cheng J, Zhang H, et al. Comparison among the imaging characteristics of the intravitreous wooden foreign body in rabbits. *Int J Clin Exp Med* 2017; 10: 2450–2459.
3. Bowser BA, Campeau NG, Carr CM, et al. Incidental ferumoxytol artifacts in clinical brain MR imaging. *Neuroradiology* 2016; 58: 1087–1091.
4. Cho WK, Ko AC, Eatamadi H, et al. Orbital and orbitocranial trauma from pencil fragments: role of timely diagnosis and management. *Am J Ophthalmol* 2017; 180: 46–54.
5. Nagae LM, Katowitz WR, Bilaniuk LT, et al. Radiological detection of intraorbital wooden foreign bodies. *Pediatr Emerg Care* 2011; 27: 895–896.
6. Zhang Y, Cheng JL, Bai J, et al. Tiny ferromagnetic intraocular foreign bodies detected by magnetic resonance imaging: a report of two cases. *J Magn Reson Imaging* 2009; 29: 704–707.
7. Liu S, Buch S, Chen Y, et al. Susceptibility-weighted imaging: current status and future directions. *NMR Biomed* 2017; 30: e3552.